Hindawi Publishing Corporation
International Journal of Antennas and Propagation
Volume 2016, Article ID 4758486, 15 pages
http://dx.doi.org/10.1155/2016/4758486

Research Article

A Tuning Computation Technique for a Multiple-Antenna-Port and Multiple-User-Port Antenna Tuner

Frédéric Broydé and Evelyne Clavelier

Excem, 12 Chemin des Hauts de Clairefontaine, 78580 Maule, France

Correspondence should be addressed to Evelyne Clavelier; eclavelier@eurexcem.com

Received 27 April 2016; Revised 13 July 2016; Accepted 7 August 2016

Academic Editor: Giuseppe Mazzarella

A multiple-user-port antenna tuner having the structure of a multidimensional π-network has recently been disclosed, together with design equations which assume lossless circuit elements. This paper is about the design of this type of antenna tuner, when losses are taken into account in each circuit element of the antenna tuner. The problem to be solved is the tuning computation, the intended results of which are the reactance values of the adjustable impedance devices of the antenna tuner, which provide an ideal match, if such reactance values exist. An efficient iterative tuning computation technique is presented and demonstrated.

1. Introduction

A multiple-antenna-port and multiple-user-port (MAPMUP) antenna tuner is intended to be inserted between several antennas and a radio device which uses these antennas simultaneously in the same frequency band [1–3]. The radio device may be a receiver, a transmitter, or a transceiver for single-user MIMO radio communication, and the antenna tuner is typically adjusted automatically [4–6]. Figure 1 shows how n antennas may be coupled to a MAPMUP antenna tuner having n antenna ports and m user ports (also referred to as "radio ports") intended to be coupled to the radio device.

In a frequency band of intended operation, with respect to the antenna ports and the user ports, the antenna tuner must behave as a passive linear device and its losses should be as low as possible. The antenna ports see an impedance matrix $\mathbf{Z}_{\mathrm{Sant}}$ of size $n \times n$ and the user ports present an impedance matrix $\mathbf{Z}_U$ of size $m \times m$. A MAPMUP antenna tuner comprises p adjustable impedance devices, each of which may be any component having two terminals which behave as the terminals of a passive linear two-terminal circuit element and which present a reactance which is adjustable by mechanical or electrical means. The function of the antenna tuner is to allow an adjustment of $\mathbf{Z}_U$, using a selection of the reactance values of its adjustable impedance devices, so as to obtain or approximate a wanted impedance matrix $\mathbf{Z}_{UW}$. This tuning capability differentiates a MAPMUP antenna tuner from a MAPMUP matching network [7–13]. Some aspects of the tuning capability of MAPMUP antenna tuners are covered in [14], which shows that the need for a suitable tuning capability (such as a full tuning capability) makes the design of a MAPMUP antenna tuner completely different from the design of a MAPMUP matching network.

A MAPMUP antenna tuner having the structure of a multidimensional π-network has recently been described [14–16]. This antenna tuner is scalable to any $n = m \geq 1$, unlike earlier MAPMUP antenna tuners. It is shown in Figure 2 for the case $n = m = 4$. The case $n = m = 1$ corresponds to a classical single-antenna-port and single-user-port (SAPSUP) antenna tuner having the structure of a π-network.

This paper is about the design of this type of MAPMUP antenna tuner. The problem to be solved is the tuning computation, the intended results of which are the adjustable impedance device reactance values which provide an ideal match $\mathbf{Z}_U = \mathbf{Z}_{UW}$, if such reactance values exist. For a lossless multidimensional π-network antenna tuner, a set of closed-form tuning computation formulas was proven in [16]. In this paper, we shall present an efficient iterative tuning computation technique, which can be used when losses are present in the circuit element of the antenna tuner. Section 2

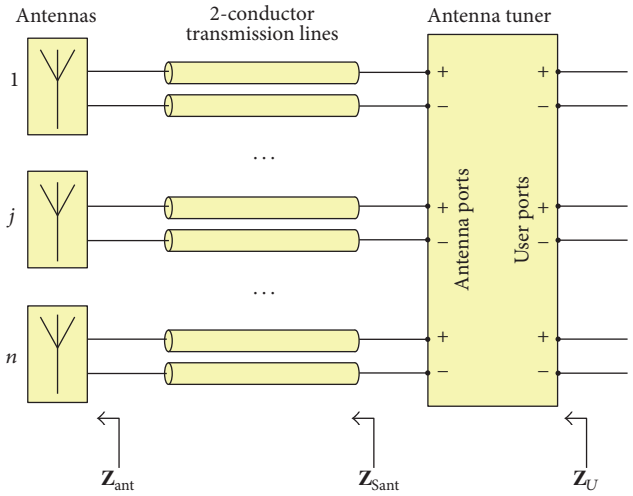

Figure 1: An array of n antennas coupled to a MAPMUP antenna tuner through n uncoupled 2-conductor transmission lines.

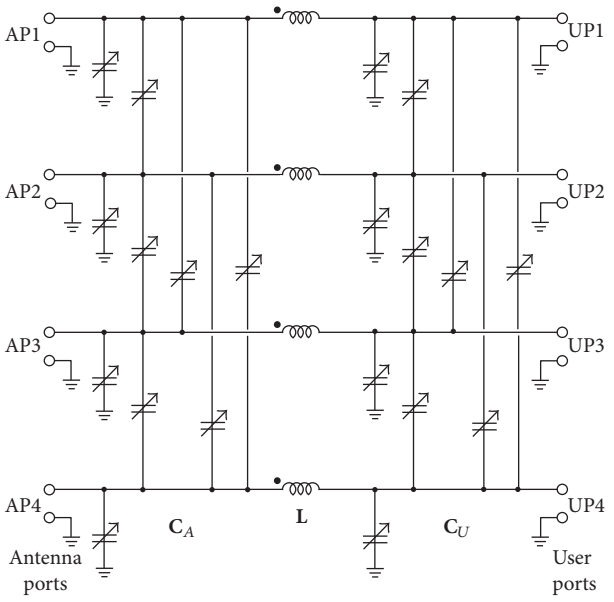

Figure 2: The MAPMUP antenna tuner having the structure of a multidimensional π-network, in a configuration having $n = 4$ antenna ports, labeled AP1 to AP4, and $m = 4$ user ports, labeled UP1 to UP4.

presents a tuning computation problem and the solution obtained for a lossless multidimensional π-network antenna tuner. Sections 3 and 4 explain the theory of the iterative algorithm. Sections 5 and 7 present solutions to the problem of Section 2, for different losses in the circuit elements. Sections 6 and 8 explore the main characteristics of the MAPMUP antenna tuner obtained in Section 5.

2. A Tuning Computation Problem

A circular antenna array is made up of $n = 4$ side-by-side parallel dipole antennas, each having a total length of

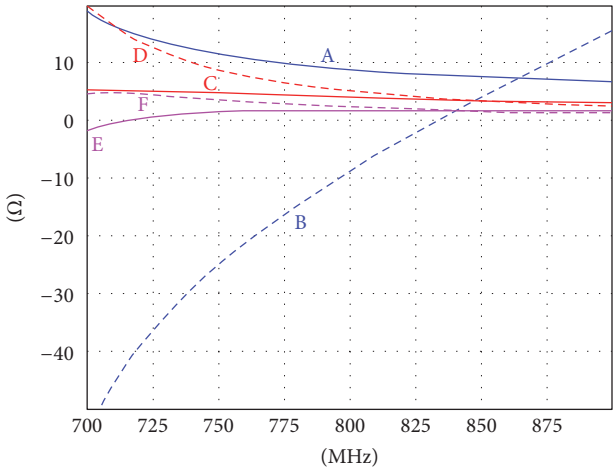

Figure 3: Entries of $\mathbf{Z}_{\text{Sant}}$ versus frequency: $\text{Re}(\mathbf{Z}_{\text{Sant }11})$ is curve A; $\text{Im}(\mathbf{Z}_{\text{Sant }11})$ is curve B; $\text{Re}(\mathbf{Z}_{\text{Sant }12})$ is curve C; $\text{Im}(\mathbf{Z}_{\text{Sant }12})$ is curve D; $\text{Re}(\mathbf{Z}_{\text{Sant }13})$ is curve E; $\text{Im}(\mathbf{Z}_{\text{Sant }13})$ is curve F.

224.8 mm. The radius of the array is 56.2 mm. Each antenna is lossless and has a 60 mm long lossy feeder. The antenna array is intended to operate in the frequency band 700 MHz to 900 MHz. At the center frequency $f_c = 800$ MHz, $\mathbf{Z}_{\text{Sant}}$ is approximately given by

$$\mathbf{Z}_{\text{Sant}} \approx \begin{pmatrix} 8.6 - 8.9j & 3.8 + 4.9j & 1.7 + 2.2j & 3.8 + 4.9j \\ 3.8 + 4.9j & 8.6 - 8.9j & 3.8 + 4.9j & 1.7 + 2.2j \\ 1.7 + 2.2j & 3.8 + 4.9j & 8.6 - 8.9j & 3.8 + 4.9j \\ 3.8 + 4.9j & 1.7 + 2.2j & 3.8 + 4.9j & 8.6 - 8.9j \end{pmatrix} \Omega. \quad (1)$$

At any frequency, $\mathbf{Z}_{\text{Sant}}$ is symmetric and circulant, as shown in (1) at f_c, so that $\mathbf{Z}_{\text{Sant}}$ is fully determined by the first three entries of its first row. These entries are plotted in the frequency range 700 MHz to 900 MHz, in Figure 3.

The MAPMUP antenna tuner of Figure 2 is used to obtain (if possible) that, at any tuning frequency f_T in this frequency range, $\mathbf{Z}_U$ approximates the wanted impedance matrix $\mathbf{Z}_{UW}$, given by

$$\mathbf{Z}_{UW} = r_0 \mathbf{1}_4, \quad (2)$$

where $r_0 = 50\,\Omega$ and where, for a positive integer q, we use $\mathbf{1}_q$ to denote the identity matrix of size $q \times q$.

Let $\mathbf{L}$ be the inductance matrix of the coils shown in Figure 2. Let $\mathbf{C}_A$ and $\mathbf{C}_U$ be the capacitance matrices of the adjustable impedance devices shown on the left and on the right, respectively, in Figure 2. In [16], formulas for the tuning computation were derived, for a lossless multidimensional π-network MAPMUP antenna tuner. In this calculation, one of

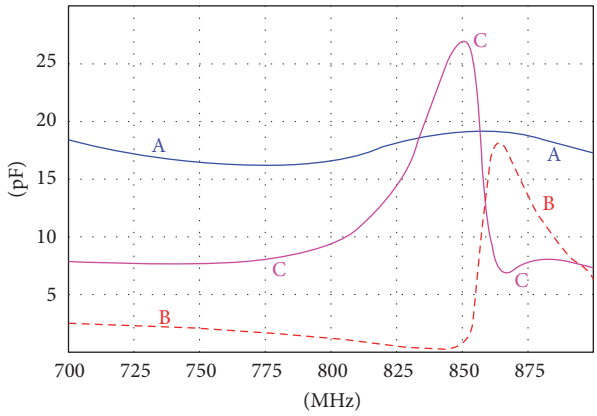

FIGURE 4: Capacitances of the adjustable impedance devices which realize $\mathbf{C}_A$ in the lossless MAPMUP antenna tuner: C_{AG} is curve A; C_{AN} is curve B; and C_{AF} is curve C.

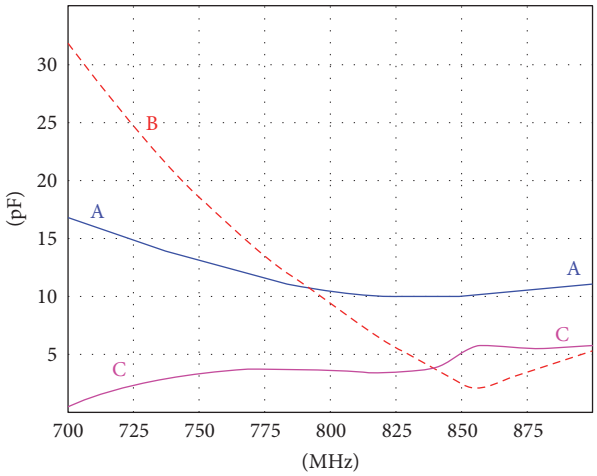

FIGURE 5: Capacitances of the adjustable impedance devices which realize $\mathbf{C}_U$ in the lossless MAPMUP antenna tuner: C_{UG} is curve A; C_{UN} is curve B; and C_{UF} is curve C.

the matrices $\mathbf{L}$, $\mathbf{C}_A$, and $\mathbf{C}_U$ is arbitrary. Let us, for instance, posit

$$\mathbf{L} \approx \begin{pmatrix} 2.700 & 0.760 & 0.850 & 0.760 \\ 0.760 & 2.700 & 0.760 & 0.850 \\ 0.850 & 0.760 & 2.700 & 0.760 \\ 0.760 & 0.850 & 0.760 & 2.700 \end{pmatrix} \text{nH}. \tag{3}$$

The purpose of the tuning computation is to determine values of $\mathbf{C}_A$ and $\mathbf{C}_U$ providing the ideal match $\mathbf{Z}_U = \mathbf{Z}_{UW}$, as a function of the tuning frequency. If we ignore losses in the circuit element of the antenna tuner, we can use (3) and formulas (7) and (9) of [16], to obtain $\mathbf{C}_A$ and $\mathbf{C}_U$. Each value of $\mathbf{C}_A$ is symmetric and circulant. Thus, it corresponds to 3 values of the capacitances of the 10 adjustable impedance devices coupled to one of the antenna ports: C_{AG} for the 4 grounded adjustable impedance devices, C_{AN} for 4 others, and C_{AF} for the 2 remaining ones. These 3 values are plotted in Figure 4, versus the tuning frequency. In the same way, each value of $\mathbf{C}_U$ is symmetric and circulant, so that it corresponds to 3 values of the capacitances of the 10 adjustable impedance devices coupled to one of the user ports: C_{UG} for the 4 grounded adjustable impedance devices, C_{UN} for 4 others, and C_{UF} for the 2 remaining ones. These 3 values are plotted in Figure 5, versus the tuning frequency.

The tuning computation problem addressed in the next sections is the computation, for the MAPMUP antenna tuner of Figure 2, in the presence of losses in the coils and in the adjustable impedance devices, of $\mathbf{C}_A$ and $\mathbf{C}_U$ providing the ideal match $\mathbf{Z}_U = \mathbf{Z}_{UW}$ at different frequencies.

3. Equations of the Tuning Computation Problem

In this section, we present the equations of the tuning computation problem. We use $\mathbf{C}_A$ and $\mathbf{G}_B$ to denote the capacitance and conductance matrices of the $m(m+1)/2$ adjustable impedance devices coupled to one of the antenna ports, so that their admittance matrix is $\mathbf{G}_B + j\omega\mathbf{C}_A$. We use $\mathbf{C}_U$ and $\mathbf{G}_V$ to denote the capacitance and conductance matrices of the $m(m+1)/2$ adjustable impedance devices coupled to one of the user ports, so that their admittance matrix is $\mathbf{G}_V + j\omega\mathbf{C}_U$. We use $\mathbf{L}$ and $\mathbf{R}$ to denote the inductance and resistance matrices of the coils, so that their impedance matrix is $\mathbf{R} + j\omega\mathbf{L}$. Since $\mathbf{C}_A$ and $\mathbf{C}_U$ are adjustable, we consider that $\mathbf{G}_B$ depends on $\mathbf{C}_A$ and on the frequency and that $\mathbf{G}_V$ depends on $\mathbf{C}_U$ and on the frequency. Since different choices of coils at the design stage, to obtain different values of $\mathbf{L}$, entail different losses, we may consider that $\mathbf{R}$ depends on $\mathbf{L}$ and on the frequency.

We use $\mathbf{G}_{\text{Sant}}$ and $\mathbf{B}_{\text{Sant}}$ to denote the conductance matrix and the susceptance matrix seen by the antenna ports so that $\mathbf{Z}_{\text{Sant}}^{-1} = \mathbf{G}_{\text{Sant}} + j\mathbf{B}_{\text{Sant}}$. We see that $\mathbf{Z}_U$ is given by

$$\mathbf{Z}_U = \left[\left[\left[\mathbf{Z}_{\text{Sant}}^{-1} + j\omega\mathbf{C}_A + \mathbf{G}_B\right]^{-1} + j\omega\mathbf{L} + \mathbf{R}\right]^{-1} + j\omega\mathbf{C}_U + \mathbf{G}_V\right]^{-1}. \tag{4}$$

We want to solve the problem of finding $\mathbf{C}_A$, $\mathbf{L}$, and $\mathbf{C}_U$ such that

$$\mathbf{Z}_U = r_0 \mathbf{1}_m, \tag{5}$$

where r_0 is a resistance. The equation to be solved is

$$g_0 \mathbf{1}_m - j\omega\mathbf{C}_U - \mathbf{G}_V = \left[\left[\mathbf{Z}_{\text{Sant}}^{-1} + j\omega\mathbf{C}_A + \mathbf{G}_B\right]^{-1} + j\omega\mathbf{L} + \mathbf{R}\right]^{-1}, \tag{6}$$

where $g_0 = 1/r_0$. Let us introduce the real matrices $\mathbf{G}_T$ and $\mathbf{B}_T$ which satisfy

$$\mathbf{G}_T + j\mathbf{B}_T = \mathbf{Z}_{\text{Sant}}^{-1} + j\omega\mathbf{C}_A + \mathbf{G}_B = \mathbf{G}_{\text{Sant}} + \mathbf{G}_B + j\left[\mathbf{B}_{\text{Sant}} + \omega\mathbf{C}_A\right] \tag{7}$$

so that (6) becomes

$$\begin{aligned} g_0\mathbf{1}_m - j\omega\mathbf{C}_U - \mathbf{G}_V &= \left(j\omega\mathbf{L} + \mathbf{R} + \left[\mathbf{G}_T + j\mathbf{B}_T\right]^{-1}\right)^{-1} \\ &= \left(\left[\mathbf{1}_m + \left(j\omega\mathbf{L} + \mathbf{R}\right)\left(\mathbf{G}_T + j\mathbf{B}_T\right)\right]\left[\mathbf{G}_T + j\mathbf{B}_T\right]^{-1}\right)^{-1} \\ &= \left(\mathbf{G}_T + j\mathbf{B}_T\right) \\ &\cdot \left(\mathbf{1}_m + \mathbf{R}\mathbf{G}_T - \omega\mathbf{L}\mathbf{B}_T + j\left[\mathbf{R}\mathbf{B}_T + \omega\mathbf{L}\mathbf{G}_T\right]\right)^{-1}. \end{aligned} \tag{8}$$

As shown in Appendix of [16], if $\mathbf{M}$ and $\mathbf{N}$ are two square real matrices of size $m \times m$ such that $\mathbf{M} + j\mathbf{N}$ and $\mathbf{M}$ are invertible, we have

$$\left(\mathbf{M} + j\mathbf{N}\right)^{-1} = \left(\mathbf{1}_m - j\mathbf{M}^{-1}\mathbf{N}\right)\left(\mathbf{M} + \mathbf{N}\mathbf{M}^{-1}\mathbf{N}\right)^{-1}. \tag{9}$$

It follows that (8) becomes

$$\begin{aligned} &g_0\mathbf{1}_m - j\omega\mathbf{C}_U - \mathbf{G}_V \\ &\quad = \left(\mathbf{G}_T + j\mathbf{B}_T\right)\left(\mathbf{1}_m - j\mathbf{M}^{-1}\mathbf{N}\right)\left(\mathbf{M} + \mathbf{N}\mathbf{M}^{-1}\mathbf{N}\right)^{-1}, \end{aligned} \tag{10}$$

where

$$\begin{aligned} \mathbf{M} &= \mathbf{1}_m + \mathbf{R}\mathbf{G}_T - \omega\mathbf{L}\mathbf{B}_T \\ \mathbf{N} &= \mathbf{R}\mathbf{B}_T + \omega\mathbf{L}\mathbf{G}_T. \end{aligned} \tag{11}$$

Thus, (6) is equivalent to

$$g_0\mathbf{1}_m - \mathbf{G}_V = \left(\mathbf{G}_T + \mathbf{B}_T\mathbf{M}^{-1}\mathbf{N}\right)\left(\mathbf{M} + \mathbf{N}\mathbf{M}^{-1}\mathbf{N}\right)^{-1} \tag{12}$$

and

$$\omega\mathbf{C}_U = \left(\mathbf{G}_T\mathbf{M}^{-1}\mathbf{N} - \mathbf{B}_T\right)\left(\mathbf{M} + \mathbf{N}\mathbf{M}^{-1}\mathbf{N}\right)^{-1}. \tag{13}$$

At this stage, we have separated the nonlinear complex matrix equation (6) into the coupled nonlinear real matrix equations (12) and (13). For a known $\mathbf{L}$, $\mathbf{R}$ is also known, so that the unknowns are $\mathbf{C}_A$ and $\mathbf{C}_U$. The left-hand sides of (12) and (13) depend only on $\mathbf{C}_U$ and their right-hand sides depend only on $\mathbf{C}_A$. We see that if $\mathbf{G}_V$ was independent of $\mathbf{C}_U$, (12) and (13) would be uncoupled because (12) could be solved to obtain $\mathbf{C}_A$ and (13) could be used to directly compute $\mathbf{C}_U$. Thus, we can say that (12) and (13) are coupled because $\mathbf{G}_V$ depends on $\mathbf{C}_U$. In the case $m = 1$, (12) and (13) may be simplified as shown in Appendix A.

4. Iterative Tuning Computation Technique

An antenna tuner makes sense only if losses are small in the adjustable impedance devices, that is, only if $\|\omega\mathbf{C}_A\|_\infty \gg \|\mathbf{G}_B\|_\infty$, $\|\mathbf{G}_{\text{Sant}}\|_\infty \gg \|\mathbf{G}_B\|_\infty$, $\|\omega\mathbf{C}_U\|_\infty \gg \|\mathbf{G}_V\|_\infty$, and $g_0 \gg \|\mathbf{G}_V\|_\infty$, where $\|\mathbf{A}\|_\infty$ is the maximum row sum matrix norm of a matrix $\mathbf{A}$ [17, § 5.6.5]. Appendix B explains in detail the tuning computation algorithm which will now be concisely presented.

We shall need an equation which gives a possible solution of (12) in the special case $\mathbf{R} = \mathbf{0}\,\Omega$ and $\mathbf{G}_B = \mathbf{G}_V = \mathbf{0}$ S (that is to say, for a lossless antenna tuner):

$$\mathbf{B}_T = (\omega\mathbf{L})^{-1} + \mathbf{G}_A\left[r_0\mathbf{G}_A^{-1}(\omega\mathbf{L})^{-2} - \mathbf{1}_m\right]^{1/2}. \tag{14}$$

This equation is a consequence of (B.8) of Appendix B, but it is also equation (26) of [16].

We shall also need an equation derived in Appendix B, which gives a possible general solution of (12):

$$\begin{aligned} \mathbf{B}_T = (\omega\mathbf{L})^{-1}\Big(&\mathbf{1}_m + \mathbf{R}\mathbf{G}_T \\ &\pm \mathbf{N}\left[\mathbf{N}^{-1}\left(g_0\mathbf{1}_m - \mathbf{G}_V\right)^{-1}\left(\mathbf{G}_T\mathbf{N}^{-1}\mathbf{M} + \mathbf{B}_T\right)\right. \\ &\left. - \mathbf{1}_m\right]^{1/2}\Big). \end{aligned} \tag{15}$$

In (14) and (15) and in Appendix B, the power 1/2 of a matrix denotes any square root [18, § 6.4.12], such as the primary matrix function associated with a suitable choice of square root in $\mathbb{C}$, this principal matrix function being defined for any nonsingular matrix [18, § 6.2.14]. We note that, unlike (14), (15) cannot be used to directly compute $\mathbf{B}_T$, because

(i) according to (11), $\mathbf{M}$ and $\mathbf{N}$ depend on $\mathbf{B}_T$;

(ii) $\mathbf{G}_V$ depends on $\mathbf{C}_U$ which by (13) depends on $\mathbf{B}_T$;

(iii) by (7), $\mathbf{G}_T$ depends on $\mathbf{G}_B$, which depends on $\mathbf{C}_A$, which again by (7) depends on $\mathbf{B}_T$.

The algorithm is shown in the box "Algorithm 1." At each step $k \geq 0$ in the iteration, there is no guaranty that $\mathbf{C}_A{}^{(k)}$ and $\mathbf{C}_U{}^{(k)}$ are real and that they are positive definite. At each step $k \geq 0$ in the iteration, we compute $F(\mathbf{Z}_U{}^{(k)})$, where we use $\mathbf{Z}_U{}^{(k)}$ to denote the value of $\mathbf{Z}_U$ given by (4) for $\mathbf{C}_A = \mathbf{C}_A{}^{(k)}$, $\mathbf{G}_B = \mathbf{G}_B(\mathbf{C}_A{}^{(k)})$, $\mathbf{C}_U = \mathbf{C}_U{}^{(k)}$, and $\mathbf{G}_V = \mathbf{G}_V(\mathbf{C}_U{}^{(k)})$ and where, for an arbitrary impedance matrix $\mathbf{Z}$ of size $q \times q$, the return figure $F(\mathbf{Z})$ is defined by [14, § VI]

$$F(\mathbf{Z}) = \|\mathbf{S}(\mathbf{Z})\|_2, \tag{16}$$

where

$$\begin{aligned} \mathbf{S}(\mathbf{Z}) &= \left(\mathbf{Z} + r_0\mathbf{I}_q\right)^{-1}\left(\mathbf{Z} - r_0\mathbf{I}_q\right) \\ &= \left(\mathbf{Z} - r_0\mathbf{I}_q\right)\left(\mathbf{Z} + r_0\mathbf{I}_q\right)^{-1} \end{aligned} \tag{17}$$

and the spectral norm $\|\mathbf{A}\|_2$ of a square matrix $\mathbf{A}$ is the largest singular value of $\mathbf{A}$ [17, § 5.6.6]. A sufficiently small value of $F(\mathbf{Z}_U{}^{(k)})$ ends the iteration. In Algorithm 1, the sufficiently small value is 10^{-4}.

A setting of each adjustable impedance device corresponds to frequency dependent values $\mathbf{C}_A$, $\mathbf{G}_B$, $\mathbf{C}_U$, and $\mathbf{G}_V$. At the end of the algorithm, we compute nominal values of $\mathbf{C}_A$ and $\mathbf{C}_U$, which are frequency independent matrices which correspond to a setting of each adjustable impedance device such that the computed values of $\mathbf{C}_A$ and $\mathbf{C}_U$ are obtained at the frequency of operation.

The selection of different square roots in (14) and (15) can be used to obtain different solutions. Appendix C shows how the iterative algorithm can be simplified in the special case $m = 1$.

Input: frequency of operation, $\mathbf{Z}_{\text{Sant}}$.
Output: approximate nominal values of $\mathbf{C}_A$ and $\mathbf{C}_U$, maximal value of the index k, and resulting $F(\mathbf{Z}_U{}^{(k)})$.
(1) compute $\mathbf{C}_A{}^{(0)}$ as the value of $\mathbf{C}_A$ given by (14) and then (7) in which $\mathbf{R} = \mathbf{0}\,\Omega$ and $\mathbf{G}_B = \mathbf{G}_V = \mathbf{0}\,\text{S}$
(2) compute $\mathbf{C}_U{}^{(0)}$ as the value of $\mathbf{C}_U$ given by (7), (11) and (13) in which $\mathbf{R} = \mathbf{0}\,\Omega$, $\mathbf{G}_B = \mathbf{0}\,\text{S}$ and $\mathbf{C}_A = \mathbf{C}_A{}^{(0)}$
(3) $k \leftarrow 0$
(4) compute $F(\mathbf{Z}_U{}^{(0)})$
(5) while $(k < 25) \wedge (F(\mathbf{Z}_U{}^{(k)}) > 10^{-4})$
(6) $k \leftarrow k + 1$
(7) compute $\mathbf{C}_A{}^{(k)}$ as the value of $\mathbf{C}_A$ given by (7), (11) and (15) in which $\mathbf{G}_B = \mathbf{G}_B(\mathbf{C}_A{}^{(k-1)})$ and $\mathbf{G}_V = \mathbf{G}_V(\mathbf{C}_U{}^{(k-1)})$, and in which, except in the left hand side of (15), $\mathbf{C}_A = \mathbf{C}_A{}^{(k-1)}$
(8) compute $\mathbf{C}_U{}^{(k)}$ as the value of $\mathbf{C}_U$ given by (7), (11) and (13) in which $\mathbf{G}_B = \mathbf{G}_B(\mathbf{C}_A{}^{(k-1)})$ and $\mathbf{C}_A = \mathbf{C}_A{}^{(k)}$
(9) compute $F(\mathbf{Z}_U{}^{(k)})$
(10) compute the nominal value of $\mathbf{C}_A$ corresponding to $\mathbf{C}_A{}^{(k)}$ at the frequency of operation
(11) compute the nominal value of $\mathbf{C}_U$ corresponding to $\mathbf{C}_U{}^{(k)}$ at the frequency of operation
(12) return said nominal value of $\mathbf{C}_A$, said nominal value of $\mathbf{C}_U$, k and $F(\mathbf{Z}_U{}^{(k)})$

Algorithm 1: Iterative algorithm for computing approximate nominal values of $\mathbf{C}_A$ and $\mathbf{C}_U$.

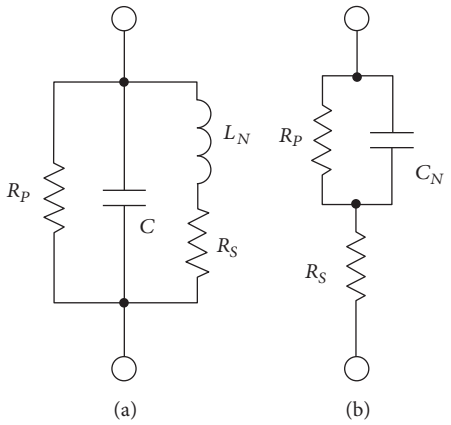

Figure 6: Equivalent circuits (a) for lossy winding of nominal inductance L_N and (b) for a lossy voltage-controlled capacitor of nominal capacitance C_N.

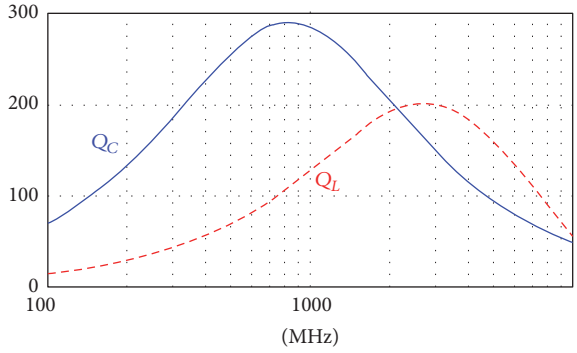

Figure 7: Quality factor Q_L of the diagonal entries of the impedance matrix $\mathbf{Z}_L$ and quality factor Q_C of all entries of the admittance matrix $\mathbf{Y}_C$, for the antenna tuner of Section 5.

5. First Tuning Computation

We use a lossy coil model based on the equivalent circuit shown in Figure 6(a). According to this model, a winding of nominal inductance L_N has an impedance which is given by

$$Z_L = \frac{1}{\left(1/\left(j\omega L_N + R_S\right)\right) + j\omega C + \left(1/R_P\right)}. \tag{18}$$

In this section, we use $L_N = 2.7\,\text{nH}$, $R_S \approx 119\,\text{m}\Omega$, $R_P \approx 20.7\,\text{k}\Omega$, and $C \approx 48.8\,\text{fF}$, these parameters being realistic for a high-Q coil. Our model of coupled lossy windings has an impedance matrix $\mathbf{Z}_L$ in which the diagonal entries are impedances given by (18) and the nondiagonal entries are produced by frequency independent mutual inductances. We have used

$$\begin{aligned}\mathbf{Z}_L &= j\omega\mathbf{L} + \mathbf{R} \\ &= Z_L\mathbf{1}_m + j\omega \begin{pmatrix} 0 & 0.76 & 0.85 & 0.76 \\ 0.76 & 0 & 0.76 & 0.85 \\ 0.85 & 0.76 & 0 & 0.76 \\ 0.76 & 0.85 & 0.76 & 0 \end{pmatrix} \text{nH}.\end{aligned} \tag{19}$$

Figure 7 shows the quality factor Q_L of the diagonal entries of the impedance matrix $\mathbf{Z}_L$. This quality factor is not very high, since it varies from about 94 to about 117 in the frequency range 700 MHz to 900 MHz.

We use an adjustable impedance device model which is based on the equivalent circuit shown in Figure 6(b).

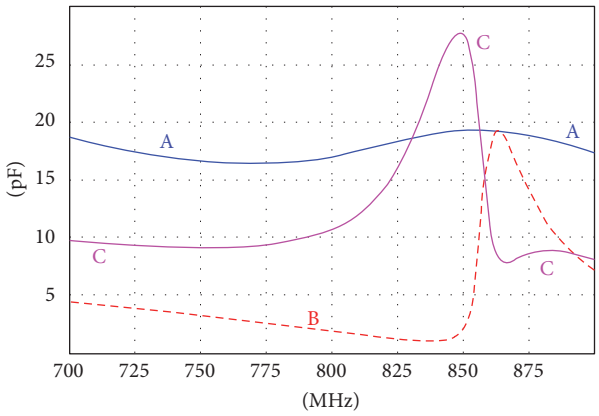

FIGURE 8: Nominal capacitances of the adjustable impedance devices which realize $\mathbf{C}_A$ in the lossy MAPMUP antenna tuner of Section 5, versus the tuning frequency: C_{AG} is curve A; C_{AN} is curve B; and C_{AF} is curve C.

According to this equivalent circuit, a capacitor of nominal capacitance C_N has an admittance which is given by

$$Y_C = \frac{C_N}{(1/(j\omega + \omega_P)) + (1/\omega_S)} \tag{20}$$

in which $1/R_P = \omega_P C_N$ and $1/R_S = \omega_S C_N$. Thus, the resulting quality factor is independent of the capacitance value. In this section, we use $\omega_P = 9 \times 10^6$ rd/s and $\omega_S = 3 \times 10^{12}$ rd/s, these parameters being reasonable for high-Q varactors. Figure 7 shows the quality factor Q_C of all entries of the admittance matrix $\mathbf{Y}_C$. In the frequency range 700 MHz to 900 MHz, this quality factor satisfies $284 < Q_C < 289$.

The losses in the coils and adjustable impedance devices are moderate in this frequency range.

To solve the problem set out in Section 2, we have used the iterative algorithm of Section 4 (Algorithm 1) to obtain the nominal values of $\mathbf{C}_A$ and $\mathbf{C}_U$, our program ending the iteration when $F(\mathbf{Z}_U)$ is less than −80 dB. Each computed nominal value of $\mathbf{C}_A$ and $\mathbf{C}_U$ is symmetric and circulant. The nominal capacitances C_{AG}, C_{AN}, and C_{AF} which realize the nominal value of $\mathbf{C}_A$, as explained in Section 2, are plotted in Figure 8, versus the tuning frequency. The nominal capacitances C_{UG}, C_{UN}, and C_{UF} which realize the nominal value of $\mathbf{C}_U$, as explained in Section 2, are plotted in Figure 9 versus the tuning frequency. The number of iterations used in the algorithm (i.e., the maximum value of k) at each tuning frequency is shown in Figure 10, and the corresponding return figure $F(\mathbf{Z})$ is shown in Figure 11. A comparison of Figure 8 with Figure 4 and of Figure 9 with Figure 5 shows large differences for $\mathbf{C}_U$ below 800 MHz. This indicates that moderate losses may strongly modify the results of the tuning computation.

Instead of an iterative algorithm, we can also consider a brute force numerical optimization to perform the tuning computation. For instance, it is possible to use $\mathbf{C}_A = \mathbf{C}_A{}^{(0)}$ and $\mathbf{C}_U = \mathbf{C}_U{}^{(0)}$ as the initial value of an optimization of the capacitances $C_{A1}, \ldots, C_{Ah}$ of the capacitors which produce

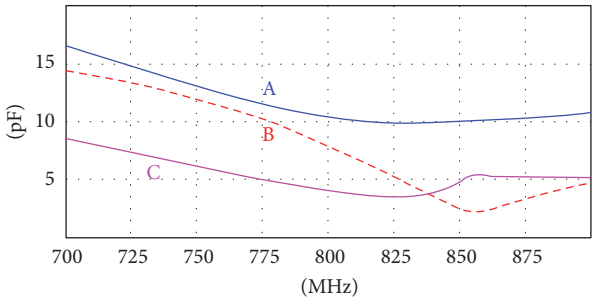

FIGURE 9: Nominal capacitances of the adjustable impedance devices which realize $\mathbf{C}_U$ in the lossy MAPMUP antenna tuner of Section 5, versus the tuning frequency: C_{UG} is curve A; C_{UN} is curve B; and C_{UF} is curve C.

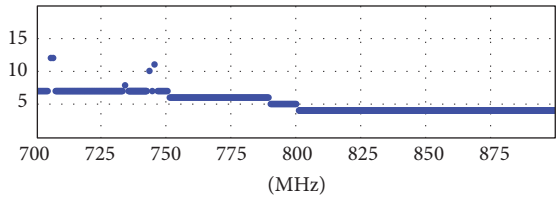

FIGURE 10: Number of iterations used in the tuning computation.

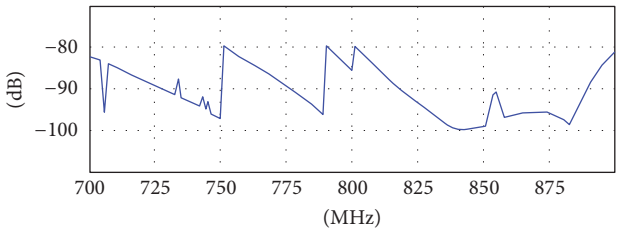

FIGURE 11: The return figure at the end of the tuning computation.

$\mathbf{C}_A$ and of the capacitances $C_{U1}, \ldots, C_{Uh}$ of the capacitors which produce $\mathbf{C}_U$, to minimize $F(\mathbf{Z}_U)$ and obtain

$$(C_{A1}, \ldots, C_{Ah}, C_{U1}, \ldots, C_{Uh}) = \underset{C_{Ai}>0,\, C_{Uj}>0}{\arg\min}\ F(\mathbf{Z}_U). \tag{21}$$

In the present case, since the symmetry of our problems requires that $\mathbf{C}_A$ and $\mathbf{C}_U$ are symmetric and circulant, we only need to consider an optimization of the 6 parameters C_{AG}, C_{AN}, C_{AF}, C_{UG}, C_{UN}, and C_{UF} defined above. We have also applied this approach to our example, using a commercially available nonlinear numerical solver, at a single frequency, because the convergence is slow. At this frequency (800 MHz), the solver does not reach the exact solution $F(\mathbf{Z}_U) = 0$, but it finds an approximate solution for which $F(\mathbf{Z}_U)$ is about −64 dB.

Moreover, if the problem did not have a rotational symmetry, the optimization approach would become unpractical, because a 20-parameter optimization would be needed (subject to the so-called "curse of dimensionality"). In contrast, the proposed iterative algorithm is unaffected by a lack of symmetry.

6. Performance of the Antenna Tuner

Let us first consider that the antenna tuner and the antennas are used for emission, a multiport source of internal impedance matrix $\mathbf{Z}_S$ being connected to the user ports. The insertion gain of the antenna tuner evaluated for $\mathbf{Z}_S = r_0\mathbf{1}_m$, denoted by G_I, is given by

$$G_I = \left.\frac{P_{\text{out}}}{P_{\text{WAT}}}\right|_{\mathbf{Z}_S=r_0\mathbf{1}_m}, \tag{22}$$

where P_{out} is the power delivered by the antenna ports of the antenna tuner to the antennas and P_{WAT} is the power received by the antennas if the antenna tuner is not present, that is, if the antennas are directly connected to the multiport source. The insertion gain is a significant measure of the benefits of the antenna tuner.

The transducer power gain of the antenna tuner evaluated for $\mathbf{Z}_S = r_0\mathbf{1}_m$, denoted by G_T, is defined as

$$G_T = \left.\frac{P_{\text{out}}}{P_{\text{ava}}}\right|_{\mathbf{Z}_S=r_0\mathbf{1}_m}, \tag{23}$$

where P_{ava} denotes the power available from the multiport source. The antenna tuner being passive, we have $G_T \leq 1$. At the tuning frequency, if $\mathbf{Z}_U$ closely approximates a wanted impedance matrix providing maximum power transfer (as is the case in Section 5, according to Figure 11), then the power received by the user ports of the antenna tuner is near P_{ava}. In this case, G_T is the efficiency of the antenna tuner.

We may define a mismatch factor without the antenna tuner evaluated for $\mathbf{Z}_S = r_0\mathbf{1}_m$, denoted by M_{WAT} and given by

$$M_{\text{WAT}} = \left.\frac{P_{\text{WAT}}}{P_{\text{ava}}}\right|_{\mathbf{Z}_S=r_0\mathbf{1}_m}. \tag{24}$$

Here, G_I, G_T, and M_{WAT} are functions of the column vector of the open-circuit voltages of the source, denoted by $\mathbf{V}_0$. More precisely G_I, G_T, and M_{WAT} are ratios of Hermitian forms of $\mathbf{V}_0$. In the case where $\mathbf{V}_0$ is known, G_I, G_T, and M_{WAT} can be computed. In the case where $\mathbf{V}_0$ is not known, it may be considered as random complex vectors. In this case, if we had suitable information on the statistics of $\mathbf{V}_0$, we could derive the expectations of G_I, G_T, and M_{WAT}. It directly follows from (22)–(24) that

$$G_I = \frac{G_T}{M_{\text{WAT}}}. \tag{25}$$

Using an antenna tuner is advantageous from the insertion gain standpoint if and only if $G_I > 1$. Since $G_T \leq 1$, by (25) the use of an antenna tuner only makes sense if M_{WAT} is sufficiently low. In Figure 12, we have plotted G_I, G_T, and M_{WAT} as a function of the tuning frequency, for the tuning

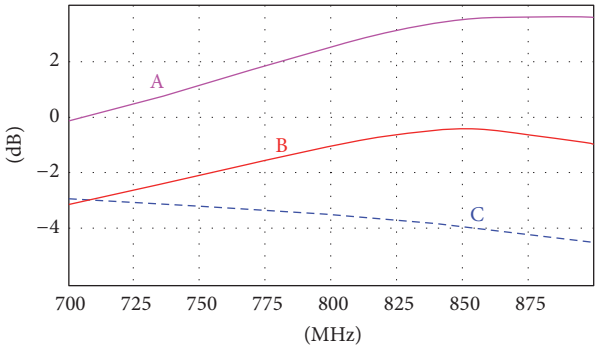

Figure 12: Insertion gain (curve A), transducer power gain (curve B), and mismatch factor without the antenna tuner (curve C).

solution shown in Figures 8 and 9, and for $\mathbf{V}_0$ equal to $\mathbf{V}_{01}$ or $\mathbf{V}_{02}$ or $\mathbf{V}_{03}$ or $\mathbf{V}_{04}$ given by

$$\begin{aligned}
\mathbf{V}_{01} &= \begin{pmatrix} 2 \\ 0 \\ 0 \\ 0 \end{pmatrix} \text{V}; \\
\mathbf{V}_{02} &= \begin{pmatrix} 0 \\ 2 \\ 0 \\ 0 \end{pmatrix} \text{V}; \\
\mathbf{V}_{03} &= \begin{pmatrix} 0 \\ 0 \\ 2 \\ 0 \end{pmatrix} \text{V}; \\
\mathbf{V}_{04} &= \begin{pmatrix} 0 \\ 0 \\ 0 \\ 2 \end{pmatrix} \text{V}
\end{aligned} \tag{26}$$

or to any multiple of any one of these vectors. The relationship (25) is visible in Figure 12. Since the insertion gain is greater than 0 dB in most of the frequency band 700 MHz to 900 MHz, this antenna tuner does not seem ridiculous from the insertion gain standpoint.

For $\alpha \in \{1, \ldots, 4\}$, let $\mathbf{E}_{0\alpha}$ be the electric field radiated by the antenna array in a configuration where $\mathbf{Z}_S = r_0\mathbf{1}_m$ and $\mathbf{V}_0$ is equal to $\mathbf{V}_{0\alpha}$ given by (26), in which rms values are used. A plot of the average radiation intensity of $\mathbf{E}_{0\alpha}$ in the far field, as a function of an angle, may be referred to as a radiation pattern of user port α. Let us use a spherical coordinate system having an origin at the center of the dipole centers and a z-axis parallel to the direction of the parallel dipoles, θ being the zenith angle (i.e., the angle with respect to the z-axis) and φ being the azimuth angle, with respect to the first antenna. Thus, the dipole centers are in the plane

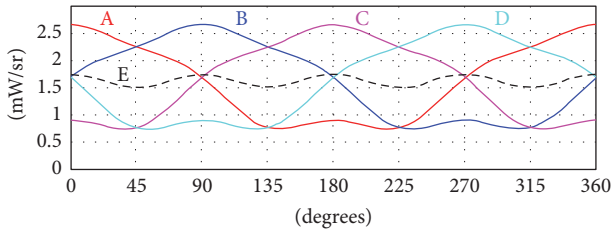

Figure 13: Radiation patterns of the user ports, at 800 MHz, in the plane $\theta = \pi/2$, versus the azimuth angle φ: the pattern of user port 1 is curve A; the pattern of user port 2 is curve B; the pattern of user port 3 is curve C; the pattern of user port 4 is curve D; and the average of curves A to D is curve E.

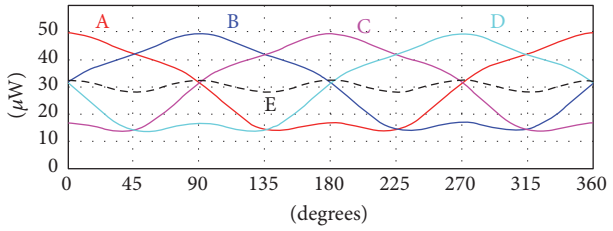

Figure 14: Reception patterns of the user ports, at 800 MHz, in the plane $\theta = \pi/2$, versus the azimuth angle φ: the pattern of user port 1 is curve A; the pattern of user port 2 is curve B; the pattern of user port 3 is curve C; the pattern of user port 4 is curve D; and the average of curves A to D is curve E.

$\theta = \pi/2$ orthogonal to the dipole antennas, which is their plane of maximum far field radiation, and the azimuths of the centers of antennas 1 to 4 are 0, $\pi/2$, π, and $3\pi/2$, respectively. Figure 13 shows the radiation patterns of the user ports, for a tuning frequency of 800 MHz and at this frequency, in the plane $\theta = \pi/2$, versus φ.

Let $\mathbf{P}_R$ be the matrix of the self- and cross and complex powers radiated by the antenna array over all values of θ and φ, defined as follows: for $\alpha \in \{1, \ldots, 4\}$ and $\beta \in \{1, \ldots, 4\}$, the entry $P_{R\alpha\beta}$ of $\mathbf{P}_R$ is given by

$$P_{R\alpha\beta} = \frac{1}{\eta_0} \int_0^{\pi} \int_0^{2\pi} \mathbf{E}_{0\alpha}^{*} \mathbf{E}_{0\beta} r^2 \sin\theta \, d\varphi \, d\theta, \tag{27}$$

where $\eta_0 \approx 376.7\,\Omega$ is the intrinsic impedance of free space, where $\mathbf{E}_{0\alpha}$ and $\mathbf{E}_{0\beta}$ are regarded as column vectors, where the star denotes the Hermitian adjoint, and where the integration is carried out at a large distance r from the antennas lying in free space. Using a numerical integration, at 800 MHz, we obtain

$$\mathbf{P}_R \approx \begin{pmatrix} 10.872 & 3.350 & -0.320 & 3.350 \\ 3.350 & 10.872 & 3.350 & -0.320 \\ -0.320 & 3.350 & 10.872 & 3.350 \\ 3.350 & -0.320 & 3.350 & 10.872 \end{pmatrix} \text{mW}. \tag{28}$$

Here, the available power of 20 mW, corresponding to any one of the $\mathbf{V}_{0\alpha}$ given by (26), leads to a power of about 15.756 mW at the output of the antenna tuner (in line with the value of G_T shown in Figure 12), but only 10.872 mW reaches the antennas and is radiated, because of feeder loss. The feeder loss of about 1.61 dB is much larger than the product of the feeder attenuation constant and the feeder length, equal to 0.20 dB at 800 MHz. This effect is similar to, but more complex than, the additional feeder loss caused by the high standing-wave ratio associated with the use of SAPSUP antenna tuners [19, ch. 3].

Since, by (27), $P_{R\alpha\beta}$ is an inner product [17, § 0.6.4] of the beams $\mathbf{E}_{0\beta}$ and $\mathbf{E}_{0\alpha}$, we can define the beam cosines $\rho_{\alpha\beta} = P_{R\alpha\beta}/(P_{R\alpha\alpha}P_{R\beta\beta})^{1/2}$ of $\mathbf{P}_R$. At 800 MHz, the matrix of these beam cosines is given by

$$\left(\rho_{\alpha\beta}\right) \approx \begin{pmatrix} 1.000 & 0.308 & -0.029 & 0.308 \\ 0.308 & 1.000 & 0.308 & -0.029 \\ -0.029 & 0.308 & 1.000 & 0.308 \\ 0.308 & -0.029 & 0.308 & 1.000 \end{pmatrix}. \tag{29}$$

Let us now consider that the antenna tuner and the antennas are used for reception, a multiport load of impedance matrix $\mathbf{Z}_L$ being connected to the user ports. Let $\mathbf{U}_0$ be the column vector of the rms voltages delivered by the user ports in a configuration where $\mathbf{Z}_L = r_0 \mathbf{1}_m$ and a plane wave of electric field amplitude 1 V/m rms impinges on the antenna array, from the direction (θ, φ) with an electric field lying in a plane containing the z-axis. A plot of the average power delivered by the user port α, as a function of an angle, may be referred to as a reception pattern of user port α. Figure 14 shows the reception patterns of the user ports, for a tuning frequency of 800 MHz and at this frequency, in the plane $\theta = \pi/2$, versus φ. The shapes of the reception patterns of the user ports correspond to those of the radiation patterns of the user ports. This is because, for each user port, the reception pattern and the radiation pattern correspond to the directivity pattern of a single-port antenna made up of all items shown in Figure 1, plus 50 Ω resistors connected to the other user ports.

Let $\mathbf{P}_D$ be the matrix of the self- and cross and complex powers delivered by the user ports, averaged over all values of θ and φ, defined as follows: for $\alpha \in \{1, \ldots, 4\}$ and $\beta \in \{1, \ldots, 4\}$, the entry $P_{D\alpha\beta}$ of $\mathbf{P}_D$ is given by

$$P_{D\alpha\beta} = \frac{1}{4\pi r_0} \int_0^{\pi} \int_0^{2\pi} U_{0\alpha} \overline{U}_{0\beta} \sin\theta \, d\varphi \, d\theta, \tag{30}$$

where the bar indicates the complex conjugate and where $U_{0\alpha}$ and $U_{0\beta}$ are entries of $\mathbf{U}_0$. Thus, it is possible to write

$$\mathbf{P}_D = \frac{1}{4\pi r_0} \int_0^{\pi} \int_0^{2\pi} \mathbf{U}_0 \mathbf{U}_0^{*} \sin\theta \, d\varphi \, d\theta. \tag{31}$$

Using a numerical integration of (31), we get

$$\mathbf{P}_D \approx \begin{pmatrix} 16.125 & 4.969 & -0.475 & 4.969 \\ 4.969 & 16.125 & 4.969 & -0.475 \\ -0.475 & 4.969 & 16.125 & 4.969 \\ 4.969 & -0.475 & 4.969 & 16.125 \end{pmatrix} \mu\text{W}. \quad (32)$$

The trace of $\mathbf{P}_D$ is the power delivered by the user ports, averaged over all directions of arrival of a plane wave of electric field amplitude 1 V/m rms impinging on the antenna array.

Since, by (30), $P_{D\alpha\beta}$ is an inner product of the beams $U_{0\alpha}$ and $U_{0\beta}$, we can define the beam cosines $P_{D\alpha\beta}/(P_{D\alpha\alpha}P_{D\beta\beta})^{1/2}$ of $\mathbf{P}_D$. In our configuration, the beam cosines of $\mathbf{P}_D$ are equal to the beam cosines of $\mathbf{P}_R$, so that they are, at 800 MHz, given by (29). We note that these beam cosines are similar to, but different from, the correlation coefficients given by (29) or (30) of [20]. The beam cosines are sometimes referred to as "orthogonality coefficients." The values of the beam cosines indicate that the beams are not far from being orthogonal, but they are not orthogonal either.

We have checked that if we remove the losses of the feeders and perform a new tuning computation for a lossless antenna tuner, we obtain a matrix of the beam cosines equal to $\mathbf{1}_4$, as requested by the theory presented in [21, 22].

7. Second Tuning Computation

We now use different parameters in the loss models of Section 5: $L_N = 2.7\,\text{nH}$, $R_S = 0.36\,\Omega$, $R_P \approx 10.1\,\text{k}\Omega$, $C \approx 93.8\,\text{fF}$, $\omega_P = 37 \times 10^6$ rd/s, and $\omega_S = 650 \times 10^9$ rd/s.

Figure 15 shows the quality factor Q_L of the diagonal entries of the impedance matrix $\mathbf{Z}_L$. Unfortunately, this quality factor is not high, since it varies from about 31.6 to about 39.5 in the frequency range 700 MHz to 900 MHz. Figure 15 also shows the quality factor Q_C of all entries of the admittance matrix $\mathbf{Y}_C$. In the frequency range 700 MHz to 900 MHz, this quality factor is close to 66. Thus, the losses in the coils and adjustable impedance devices are higher than in Section 5 and very substantial. This is good for testing our iterative algorithm, because higher losses are less favorable for convergence.

We have again used the iterative algorithm of Section 4 (Algorithm 1) to obtain $\mathbf{C}_A$ and $\mathbf{C}_U$, our program ending the iteration when $F(\mathbf{Z}_U)$ is less than -80 dB. The number of iterations needed to obtain this required accuracy at each tuning frequency is shown in Figure 16, and the corresponding return figure $F(\mathbf{Z})$ is shown in Figure 17. A comparison of Figure 10 with Figure 16 shows that the number of iterations has increased. However, the algorithm still converges rapidly.

In Figure 18, we have plotted G_I, G_T, and M_{WAT} as a function of the tuning frequency, for the tuning solution obtained here, and for $\mathbf{V}_0$ equal to $\mathbf{V}_{01}$ or $\mathbf{V}_{02}$ or $\mathbf{V}_{03}$ or $\mathbf{V}_{04}$ given by (26) or to any multiple of any one of these vectors. A comparison of Figure 12 with Figure 18 shows that G_I and G_T have decreased. Since the insertion gain is below 0 dB below about 790 MHz, this antenna tuner is not satisfactory from the insertion gain standpoint.

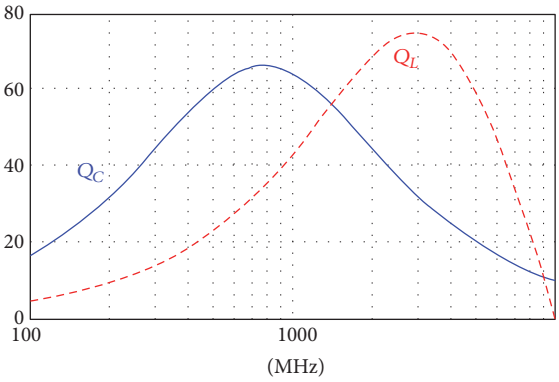

Figure 15: Quality factor Q_L of the diagonal entries of the impedance matrix $\mathbf{Z}_L$ and quality factor Q_C of all entries of the admittance matrix $\mathbf{Y}_C$, for the antenna tuner of Section 7.

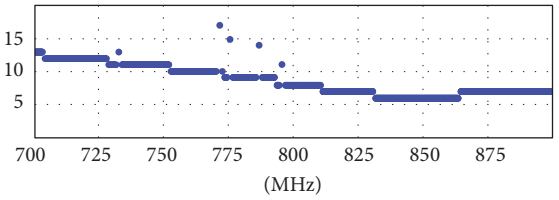

Figure 16: Number of iterations used in the tuning computation.

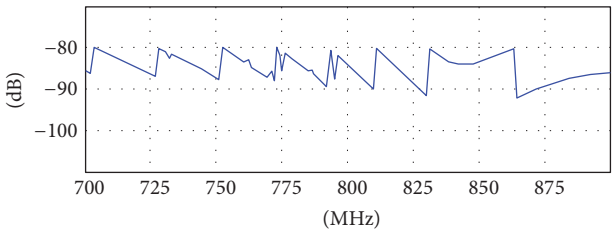

Figure 17: The return figure at the end of the tuning computation.

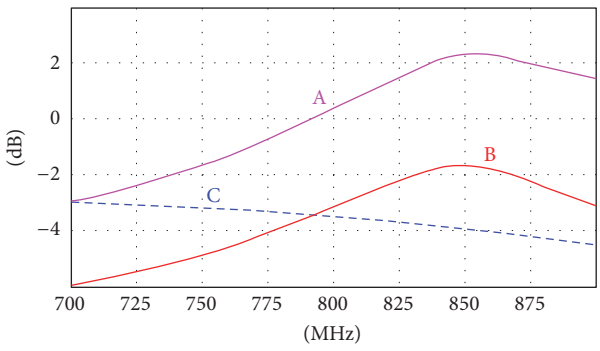

Figure 18: Insertion gain (curve A), transducer power gain (curve B), and mismatch factor without the antenna tuner (curve C).

8. Effects of Capacitance Deviations

To ensure that the tuning computation technique is applicable to real components, we now study the criticality of the

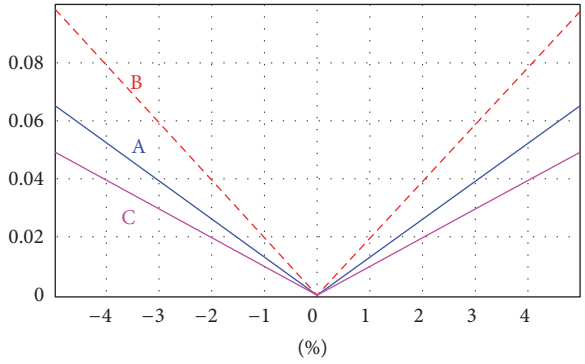

FIGURE 19: $F(\mathbf{Z}_U)$ at the tuning frequency, versus a relative capacitance variation of a single adjustable impedance device contributing to $\mathbf{C}_U$: curve A if its initial value is C_{UG}; curve B if its initial value is C_{UN}; curve C if its initial value is C_{UF}.

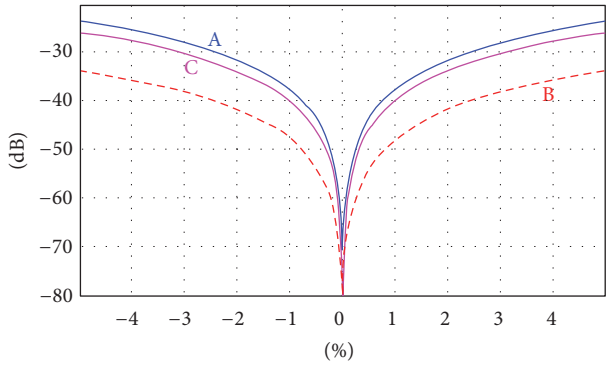

FIGURE 20: $F(\mathbf{Z}_U)$ in dB at the tuning frequency, versus a relative capacitance variation of a single adjustable impedance device contributing to $\mathbf{C}_A$: curve A if its initial value is C_{AG}; curve B if its initial value is C_{AN}; curve C if its initial value is C_{AF}.

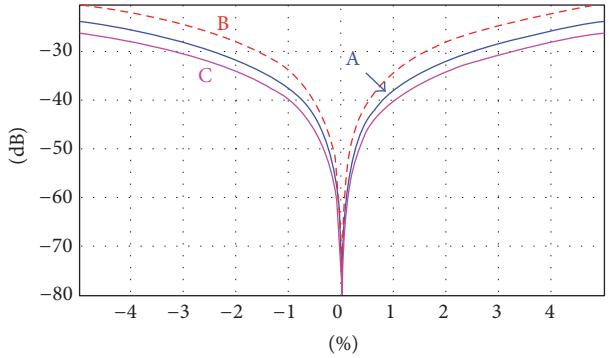

FIGURE 21: $F(\mathbf{Z}_U)$ in dB at the tuning frequency, versus a relative capacitance variation of a single adjustable impedance device contributing to $\mathbf{C}_U$: curve A if its initial value is C_{UG}; curve B if its initial value is C_{UN}; curve C if its initial value is C_{UF}.

calculated values, for the MAPMUP antenna tuner designed in Section 5. We consider deviations of one or more of the capacitances of its 20 adjustable impedance devices, from the computed ones, and we investigate the effects of the deviations on the return figure $F(\mathbf{Z}_U)$ at 800 MHz, for a tuning frequency of 800 MHz.

Since, at the tuning frequency, $F(\mathbf{Z}_U)$ practically reaches its minimum value of 0, it would, if it was differentiable, have all its partial derivatives with respect to the capacitances practically equal to zero, at the tuning frequency. Thus, each of the 20 absolute sensitivities of $F(\mathbf{Z}_U)$ with respect to the capacitance of one of the adjustable impedance devices would practically be zero, at the tuning frequency [23, ch. 68]. Figure 19 shows $F(\mathbf{Z}_U)$ at the tuning frequency, as a function of a relative capacitance variation of a single adjustable impedance device contributing to $\mathbf{C}_U$. All curves of Figure 19 have a corner point at zero relative capacitance variation. The same phenomenon occurs in plots of $F(\mathbf{Z}_U)$ at the tuning frequency, as a function of a relative capacitance variation of a single adjustable impedance device contributing to $\mathbf{C}_A$. For much smaller capacitance variations, the corner points vanish, but no useful absolute or relative sensitivity with respect to the capacitances of the adjustable impedance devices can be defined.

Figures 20 and 21 show $F(\mathbf{Z}_U)$ in dB, at the tuning frequency, as a function of a relative capacitance variation of a single adjustable impedance device contributing to $\mathbf{C}_A$ or to $\mathbf{C}_U$.

To obtain a better idea of the effect of simultaneous deviations of the capacitance of the 20 adjustable impedance devices, we have assumed independent normally distributed capacitance deviations, with a zero mean deviation from the computed values, and a specified relative standard deviation σ_C. At the tuning frequency, we have determined the statistic of $F(\mathbf{Z}_U)$ in dB, the mean of $F(\mathbf{Z}_U)$ in dB, denoted by m_F, and the corrected sample standard deviation of $F(\mathbf{Z}_U)$ in dB, denoted by σ_F. The histogram of Figure 22 shows the relative frequency of $F(\mathbf{Z}_U)$ in dB obtained for $\sigma_C = 1\%$, with 10000 samples (of the MAPMUP antenna tuner). The assumption $\sigma_C = 1\%$ could, for instance, correspond to a ±3% tolerance defined by a 3-sigma deviation. For the statistics shown in Figure 22, we have $m_F \approx -27.22$ dB and $\sigma_F \approx 2.79$ dB. The minimum value of $F(\mathbf{Z}_U)$ is −39.96 dB. It is remarkable that this minimum value is not closer to the lowest possible value of about −85.68 dB shown in Figure 11 for 800 MHz. This is because each sample comprises 20 normally distributed capacitances, so that the probability of having all of these capacitances close to their respective computed values is very small. The maximum value of $F(\mathbf{Z}_U)$ is −19.00 dB, whereas for a normal distribution the probability of having $F(\mathbf{Z}_U)$ greater than $m_F + 3\sigma_F \approx -18.86$ dB would be about 1.35×10^{-3}, corresponding to an expectation of about 13.5 for 10000 samples. Figure 23 shows m_F and σ_F, as a function of σ_C, obtained with 1000 samples for each value of σ_C.

Based on the foregoing, we may conclude that a specified maximum return figure of $m_F+3\sigma_F \approx -18.86$ dB at the tuning frequency can reliably be obtained with $\sigma_C \leq 1\%$. This value of $m_F + 3\sigma_F$ is less impressive than the return figures below −80 dB shown in Figure 11. However, this specified maximum return figure can be compared to a reasonable design target −10 dB for a wireless transmitter and to the return figure achievable with an alternative antenna tuner made up of 4

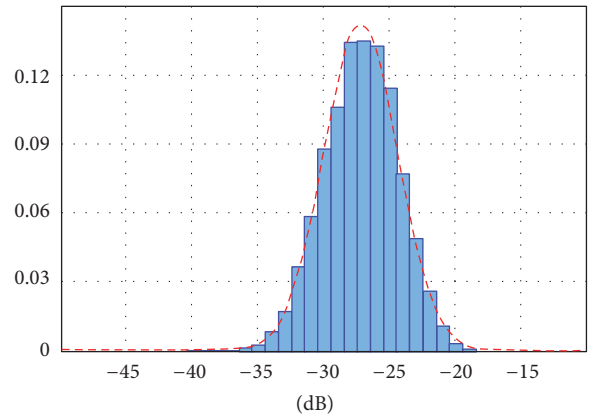

FIGURE 22: Histogram of the relative frequency of $F(\mathbf{Z}_U)$ in dB, for $\sigma_C = 1\%$, obtained with 10000 samples, and normal distribution having the same mean and the same standard deviation (dashed curve).

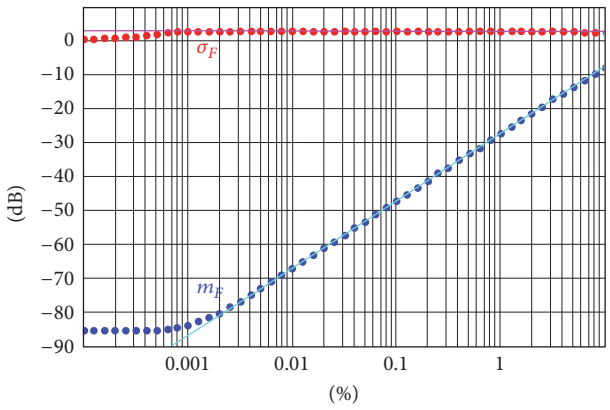

FIGURE 23: m_F and σ_F versus σ_C and linear regression lines based on the values obtained for $0.01\% \le \sigma_C \le 10\%$.

independent and uncoupled SAPSUP antenna tuners each having the structure of a π-network. Such an antenna tuner corresponds to the schematic diagram of Figure 2, with the constraint that $\mathbf{C}_A$, $\mathbf{L}$, and $\mathbf{C}_U$ are diagonal matrices. Using the same L_N and Y_C as in Section 5, we obtain, for this alternative antenna tuner, a minimum return figure of −5.90 dB at 800 MHz, obtained for nominal values of C_{AG} and C_{UG}, respectively, equal to about 25.36 pF and 24.02 pF. Thus, the specified maximum return figure is much better than the return figure achievable with the alternative antenna tuner using optimum capacitances.

The antenna tuners considered in this paper are typically intended to be adjusted automatically. In an automatic tuning system using closed-loop control, like the ones considered in [4–6], deviations of the adjustable impedance device capacitances caused by manufacturing tolerances, temperature, or other external causes may be automatically compensated. This is not the case in an automatic tuning system using open-loop control, like the ones considered in [24–26]. With open-loop control, the effects of component value variations are crucial, because they are not inherently compensated.

9. Conclusion

We have studied the design of a MAPMUP antenna tuner having the structure of a multidimensional π-network, when losses are taken into account in all circuit elements of the antenna tuner. Our work also covers a SAPSUP having the structure of a π-network. The main aspect that we have addressed is the tuning computation, the intended results of which are the adjustable impedance device reactance values which provide an ideal match of the antenna tuner, if such reactance values exist.

An efficient iterative tuning computation technique was explained and demonstrated in two examples. It can be used with circuit element losses depending in any way on the frequency and on the reactance of the circuit element. In the examples used to demonstrate the iterative tuning computation algorithm, we have chosen to use moderate losses in the first example and higher losses in the second example. The algorithm converges rapidly in both cases, but the speed decreases with increased losses. We have found that moderate losses may substantially modify the results of the tuning computation. In other words, the adjustable impedance device reactance values which provide an ideal match may, in the presence of moderate losses, be significantly different from what they would be if losses were not present.

The fact that the iterative tuning computation technique converges shows that the multidimensional π-network antenna tuner may be able to provide an ideal match $\mathbf{Z}_U = r_0\mathbf{1}_m$ which realizes decoupling and matching. In the investigated examples, this is obtained at any frequency in a wide frequency band of intended operation. The iterative tuning computation technique can be used as a tool to design π-network and multidimensional π-network antenna tuners. In addition, it can be used in automatic tuning systems based on an open-loop control scheme, such as the ones described in [24–26], to obtain the tuning control signals which determine the reactance of each of the adjustable impedance devices.

The design of a MAPMUP antenna tuner is a new field, with many unanswered questions. For instance, the selection of the inductance values of π-network and multidimensional π-network antenna tuners has not been addressed in this paper, since we have solved (12) and (13) for a known $\mathbf{L}$. The literature in this area is limited to SAPSUP π-network antenna tuners, and available design techniques (except optimization using a general-purpose circuit optimizer, which is extremely slow) ignore losses in the circuit elements of the antenna tuner or do not fully take them into account [27, 28]. We believe that this work could also be used to solve this problem, for multidimensional π-network antenna tuners, with arbitrary losses.

Appendix

A. Equations of the Tuning Computation Problem for a SAPSUP Antenna Tuner

In the case of a π-network SAPSUP antenna tuner, the results of Section 3 may be simplified as follows. Here, the antenna

port sees an impedance Z_{Sant} and the user port presents an impedance Z_U. We use C_A and G_B to denote the capacitance and the conductance of the adjustable impedance device coupled to the antenna port, so that its admittance is $G_B + j\omega C_A$. We use C_U and G_V to denote the capacitance and the conductance of the adjustable impedance device coupled to the user port, so that its admittance is $G_V + j\omega C_U$. We use L and R to denote the inductance and the resistance of the coil, so that its impedance is $R + j\omega L$. We consider that G_B depends on C_A and on the frequency, G_V depends on C_U and on the frequency, and R depends on L and on the frequency.

We use G_{Sant} and B_{Sant} to denote the conductance and the susceptance seen by the antenna port, so that $1/Z_{\text{Sant}} = G_{\text{Sant}} + jB_{\text{Sant}}$. Here, (4) becomes

$$Z_U = \left(\left(\left(Z_{\text{Sant}}^{-1} + j\omega C_A + G_B\right)^{-1} + j\omega L + R\right)^{-1} + j\omega C_U + G_V\right)^{-1}. \tag{A.1}$$

We want to solve the problem of finding C_A, L, and C_U such that Z_U is equal to a wanted resistance r_0. The equation to be solved is

$$g_0 - j\omega C_U - G_V = \left(\left(Z_{\text{Sant}}^{-1} + j\omega C_A + G_B\right)^{-1} + j\omega L + R\right)^{-1}. \tag{A.2}$$

Let us introduce the reals G_T and B_T which satisfy

$$G_T + jB_T = \frac{1}{Z_{\text{Sant}}} + j\omega C_A + G_B = G_{\text{Sant}} + G_B + j\left[B_{\text{Sant}} + \omega C_A\right]. \tag{A.3}$$

We find that (A.2) is equivalent to

$$g_0 - G_V = \frac{G_T + R\left(G_T^2 + B_T^2\right)}{\left(1 + RG_T - \omega LB_T\right)^2 + \left(RB_T + \omega LG_T\right)^2}, \tag{A.4}$$

$$\omega C_U = \frac{\omega L\left(G_T^2 + B_T^2\right) - B_T}{\left(1 + RG_T - \omega LB_T\right)^2 + \left(RB_T + \omega LG_T\right)^2} \tag{A.5}$$

which replace (12) and (13).

B. Derivation of a Tuning Computation Technique for a MAPMUP Antenna Tuner

In the case of a multidimensional π-network MAPMUP antenna tuner, the results of Section 4 may be established as follows.

Assuming that losses are small in the adjustable impedance devices, an iterative algorithm could in principle be used to solve (12) and (13): at each iteration of this algorithm, $\mathbf{C}_A$ and $\mathbf{C}_U$ are determined using (12) and (13), respectively, in which $\mathbf{G}_B$ and $\mathbf{G}_V$ are regarded as constants which are updated at each iteration, based on the values of $\mathbf{C}_A$ and $\mathbf{C}_U$ determined at the previous iteration, $\mathbf{G}_B$ and $\mathbf{G}_V$ being initially set to the null matrix of size $m \times m$.

A difficulty is that we are not able to easily compute a value of $\mathbf{C}_A$ which is a solution of (12), for arbitrary values of $\mathbf{G}_B$ and $\mathbf{G}_V$. To address this question, (12) can be manipulated to obtain

$$\begin{aligned}
&\left(g_0\mathbf{1}_m - \mathbf{G}_V\right)\left(\mathbf{M} + \mathbf{N}\mathbf{M}^{-1}\mathbf{N}\right) = \mathbf{G}_T + \mathbf{B}_T\mathbf{M}^{-1}\mathbf{N},\\
&\left(g_0\mathbf{1}_m - \mathbf{G}_V\right)\left(\mathbf{M}\mathbf{N}^{-1}\mathbf{M} + \mathbf{N}\right) = \mathbf{G}_T\mathbf{N}^{-1}\mathbf{M} + \mathbf{B}_T,\\
&\left(g_0\mathbf{1}_m - \mathbf{G}_V\right)\left(\left(\mathbf{M}\mathbf{N}^{-1}\right)^2 + \mathbf{1}_m\right)\\
&\quad = \left(\mathbf{G}_T\mathbf{N}^{-1}\mathbf{M} + \mathbf{B}_T\right)\mathbf{N}^{-1},
\end{aligned} \tag{B.1}$$

where we have assumed that $\mathbf{N}$ is invertible. Using (11), we get

$$\left(g_0\mathbf{1}_m - \mathbf{G}_V\right)\left(\left(\left(\mathbf{1}_m + \mathbf{R}\mathbf{G}_T - \omega\mathbf{L}\mathbf{B}_T\right)\mathbf{N}^{-1}\right)^2 + \mathbf{1}_m\right) = \left(\mathbf{G}_T\mathbf{N}^{-1}\mathbf{M} + \mathbf{B}_T\right)\mathbf{N}^{-1} \tag{B.2}$$

which may be manipulated to obtain

$$\left(\left(\mathbf{1}_m + \mathbf{R}\mathbf{G}_T - \omega\mathbf{L}\mathbf{B}_T\right)\mathbf{N}^{-1}\right)^2 = \left(g_0\mathbf{1}_m - \mathbf{G}_V\right)^{-1}\left(\mathbf{G}_T\mathbf{N}^{-1}\mathbf{M} + \mathbf{B}_T\right)\mathbf{N}^{-1} - \mathbf{1}_m, \tag{B.3}$$

$$\left(\mathbf{N}^{-1}\left(\mathbf{1}_m + \mathbf{R}\mathbf{G}_T - \omega\mathbf{L}\mathbf{B}_T\right)\right)^2 = \mathbf{N}^{-1}\left(g_0\mathbf{1}_m - \mathbf{G}_V\right)^{-1}\left(\mathbf{G}_T\mathbf{N}^{-1}\mathbf{M} + \mathbf{B}_T\right) - \mathbf{1}_m. \tag{B.4}$$

A possible solution of (B.4) is

$$\mathbf{1}_m + \mathbf{R}\mathbf{G}_T - \omega\mathbf{L}\mathbf{B}_T = \mp\mathbf{N}\left[\mathbf{N}^{-1}\left(g_0\mathbf{1}_m - \mathbf{G}_V\right)^{-1}\left(\mathbf{G}_T\mathbf{N}^{-1}\mathbf{M} + \mathbf{B}_T\right) - \mathbf{1}_m\right]^{1/2}. \tag{B.5}$$

Thus, a possible solution of (12) may satisfy

$$\mathbf{B}_T = (\omega\mathbf{L})^{-1}\left(\mathbf{1}_m + \mathbf{R}\mathbf{G}_T \pm \mathbf{N}\left[\mathbf{N}^{-1}\left(g_0\mathbf{1}_m - \mathbf{G}_V\right)^{-1}\left(\mathbf{G}_T\mathbf{N}^{-1}\mathbf{M} + \mathbf{B}_T\right) - \mathbf{1}_m\right]^{1/2}\right) \tag{B.6}$$

in which, according to (11), $\mathbf{N}$ unfortunately depends on $\mathbf{B}_T$. However, it may easily be shown that, in the special case where $\mathbf{R}$ is the null matrix, using (11) we get

$$\mathbf{N}\left[\mathbf{N}^{-1}\left(g_0\mathbf{1}_m - \mathbf{G}_V\right)^{-1}\left(\mathbf{G}_T\mathbf{N}^{-1}\mathbf{M} + \mathbf{B}_T\right) - \mathbf{1}_m\right]^{1/2} = \omega\mathbf{L}\mathbf{G}_T\left[\left(\omega\mathbf{L}\left(g_0\mathbf{1}_m - \mathbf{G}_V\right)\omega\mathbf{L}\mathbf{G}_T\right)^{-1} - \mathbf{1}_m\right]^{1/2} \tag{B.7}$$

so that

$$\mathbf{B}_T = (\omega\mathbf{L})^{-1} \pm \mathbf{G}_T\left[\left(\omega\mathbf{L}\left(g_0\mathbf{1}_m - \mathbf{G}_V\right)\omega\mathbf{L}\mathbf{G}_T\right)^{-1} - \mathbf{1}_m\right]^{1/2}. \tag{B.8}$$

Input: frequency of operation, Z_{Sant}.
Output: approximate nominal values of C_A and C_U, maximal value of the index k, and resulting $F(Z_U{}^{(k)})$.
(1) compute $C_A{}^{(0)}$ as the value of C_A given by (A.3) and (C.3) in which $G_B = G_V = 0$ S
(2) compute $C_U{}^{(0)}$ as the value of C_U given by (A.3) and (A.5) in which $G_B = 0$ S and $C_A = C_A{}^{(0)}$
(3) $k \leftarrow 0$
(4) compute $F(Z_U{}^{(0)})$
(5) while $(k < 25) \wedge (F(Z_U{}^{(k)}) > 10^{-4})$
(6) $\quad k \leftarrow k + 1$
(7) $\quad$ compute $C_A{}^{(k)}$ as the value of C_A given by (A.3) and (C.3) in which $G_B = G_B(C_A{}^{(k-1)})$ and $G_V = G_V(C_U{}^{(k-1)})$
(8) $\quad$ compute $C_U{}^{(k)}$ as the value of C_U given by (A.3) and (A.5) in which $G_B = G_B(C_A{}^{(k-1)})$ and $C_A = C_A{}^{(k)}$
(9) $\quad$ compute $F(Z_U{}^{(k)})$
(10) compute the nominal value of C_A corresponding to $C_A{}^{(k)}$ at the frequency of operation
(11) compute the nominal value of C_U corresponding to $C_U{}^{(k)}$ at the frequency of operation
(12) return said nominal value of C_A, said nominal value of C_U, k and $F(Z_U{}^{(k)})$

Algorithm 2: Iterative algorithm for computing approximate nominal values of C_A and C_U.

Thus, for $\mathbf{R} = \mathbf{0}\,\Omega$ the right-hand side of (B.6) does not depend on $\mathbf{B}_T$. This indicates that, for small losses in the coil, that is, for $\|\omega\mathbf{L}\|_\infty \gg \|\mathbf{R}\|_\infty$, the part of the right-hand side of (B.6) which depends on $\mathbf{B}_T$ may be treated as a small perturbation.

Thus, approximate values of $\mathbf{C}_A$, $\mathbf{G}_B$, $\mathbf{C}_U$, and $\mathbf{G}_V$ satisfying (6) can be computed using an iterative algorithm in which

(i) $\mathbf{C}_A{}^{(0)}$ is a solution of (12) obtained for $\mathbf{R} = \mathbf{0}\,\Omega$ and $\mathbf{G}_B = \mathbf{G}_V = \mathbf{0}$ S, given by (7) and (B.8), and $\mathbf{C}_U{}^{(0)}$ is given by (7), (11), and (13) in which $\mathbf{R} = \mathbf{0}\,\Omega$, $\mathbf{G}_B = \mathbf{0}$ S and $\mathbf{C}_A = \mathbf{C}_A{}^{(0)}$;

(ii) for a positive integer k, $\mathbf{C}_A{}^{(k)}$ is an *approximate* solution of (12) obtained for $\mathbf{G}_B = \mathbf{G}_B(\mathbf{C}_A{}^{(k-1)})$ and $\mathbf{G}_V = \mathbf{G}_V(\mathbf{C}_U{}^{(k-1)})$, given by (7), (11), and (B.6) in which $\mathbf{G}_B = \mathbf{G}_B(\mathbf{C}_A{}^{(k-1)})$ and $\mathbf{G}_V = \mathbf{G}_V(\mathbf{C}_U{}^{(k-1)})$ and in which, except in the left-hand side of (B.6), $\mathbf{C}_A = \mathbf{C}_A{}^{(k-1)}$, and $\mathbf{C}_U{}^{(k)}$ is given by (7), (11), and (13) in which $\mathbf{G}_B = \mathbf{G}_B(\mathbf{C}_A{}^{(k-1)})$ and $\mathbf{C}_A = \mathbf{C}_A{}^{(k)}$.

Appendix C shows how the iterative algorithm can be simplified in the special case $m = 1$.

C. Derivation of a Tuning Computation Technique for a SAPSUP Antenna Tuner

In the case of a π-network SAPSUP antenna tuner, the results of Appendix B may be simplified as follows. Here, (A.4) may be written

$$\begin{aligned}(g_0 - G_V)\left[1 + \left(R^2 + (\omega L)^2\right)\left(G_T^2 + B_T^2\right) + 2RG_T\right. \\ \left. - 2\omega L B_T\right] = G_T + R\left(G_T^2 + B_T^2\right).\end{aligned} \tag{C.1}$$

Thus, in an iterative algorithm at each step of which G_B and G_V are regarded as constant, (A.4) becomes the quadratic equation

$$\begin{aligned}&\left\{(g_0 - G_V)\left((\omega L)^2 + R^2\right) - R\right\} B_T^2 \\ &\quad - 2\omega L\,(g_0 - G_V)\,B_T \\ &\quad + (g_0 - G_V)\left\{(1 + RG_T)^2 + (\omega L G_T)^2\right\} - G_T \\ &\quad - RG_T^2 = 0\end{aligned} \tag{C.2}$$

of unknown B_T, the solutions of which are given by

$$B_T = \frac{\omega L \pm \sqrt{(\omega L)^2 - \left[(\omega L)^2 + R^2 - \left(R/\left(g_0 - G_V\right)\right)\right] \times \left[\left(1 + RG_T\right)^2 + \left(\omega L G_T\right)^2 - \left(\left(G_T + RG_T^2\right)/\left(g_0 - G_V\right)\right)\right]}}{(\omega L)^2 + R^2 - \left(R/\left(g_0 - G_V\right)\right)}. \tag{C.3}$$

Here, approximate values C_A, G_B, C_U, and G_V satisfying (A.2) can be computed using an iterative algorithm in which

(i) $C_A{}^{(0)}$ is a solution of (A.4) obtained for $G_B = G_V = 0$ S, given by (A.3) and (C.3) in which $G_B = G_V = 0$ S; and $C_U{}^{(0)}$ is given by (A.3) and (A.5) in which $C_A = C_A{}^{(0)}$ and $G_B = 0$ S;

(ii) for a positive integer k, $C_A{}^{(k)}$ is a solution of (A.4) obtained for $G_B = G_B(C_A{}^{(k-1)})$ and $G_V = G_V(C_U{}^{(k-1)})$, given by (A.3) and (C.3) in which $G_B = G_B(C_A{}^{(k-1)})$ and $G_V = G_V(C_U{}^{(k-1)})$; and $C_U{}^{(k)}$ is given by (A.3) and (A.5) in which $C_A = C_A{}^{(k)}$ and $G_B = G_B(C_A{}^{(k-1)})$.

The full algorithm is shown in the box "Algorithm 2." A major difference between this algorithm and the one proposed in Section 4 and Appendix B for the MAPMUP antenna tuner is that (C.3) is an exact solution of (A.4) for

known G_B and G_V, whereas no exact solution of (12) is available in Appendix B, except (B.8) for $\mathbf{R} = \mathbf{0}\,\Omega$.

At each step $k \geq 0$ in the iteration, there is no guaranty that ${C_A}^{(k)}$ and ${C_U}^{(k)}$ are real and that ${C_A}^{(k)} > 0$ and ${C_U}^{(k)} > 0$. At each step $k \geq 0$ in the iteration, we compute $F({Z_U}^{(k)})$, where we use ${Z_U}^{(k)}$ to denote the value of Z_U given by (A.1) for $C_A = {C_A}^{(k)}$, $G_B = G_B({C_A}^{(k)})$, $C_U = {C_U}^{(k)}$, and $G_V = G_V({C_U}^{(k)})$ and where, for an arbitrary impedance Z, the return figure $F(Z)$ is

$$F(Z) = \left|\frac{Z - r_0}{Z + r_0}\right|. \tag{C.4}$$

that is, $F(Z)$ is the absolute value of a reflection coefficient. A sufficiently small value of $F({Z_U}^{(k)})$ ends the iteration.

Competing Interests

The authors declare that they have no competing interests.

References

[1] N. Murtaza, M. Hein, and E. Zameshaeva, "Reconfigurable decoupling and matching network for a cognitive antenna," in *Proceedings of the 41st European Microwave Conference (EuMC '11)*, pp. 874–877, Manchester, UK, October 2011.

[2] X. Tang, K. Mouthaan, and J. C. Coetzee, "Tunable decoupling and matching network for diversity enhancement of closely spaced antennas," *IEEE Antennas and Wireless Propagation Letters*, vol. 11, pp. 268–271, 2012.

[3] A. Krewski and W. L. Schroeder, "Electrically tunable mode decomposition network for 2-port MIMO antennas," in *Proceedings of the 2013 Loughborough Antennas and Propagation Conference (LAPC '13)*, pp. 553–558, Loughborough, UK, November 2013.

[4] U.S. patent no. 9,337,534, "Method and device for radio reception using an antenna tuning apparatus and a plurality of antennas," Priority: French patent application 12/02564 of 27 September 2012.

[5] U.S. patent no. 9,077,317, "Method and apparatus for automatically tuning an impedance matrix, and radio transmitter using this apparatus". Priority: French patent application 13/00878 of 15 April 2013.

[6] I. Vasilev, V. Plicanic, and B. K. Lau, "Impact of antenna design on MIMO performance for compact terminals with adaptive impedance matching," *IEEE Transactions on Antennas and Propagation*, vol. 64, no. 4, pp. 1454–1465, 2016.

[7] W. P. Geren, C. R. Curry, and J. Andersen, "A practical technique for designing multiport coupling networks," *IEEE Transactions on Microwave Theory and Techniques*, vol. 44, no. 3, pp. 364–371, 1996.

[8] J. W. Wallace and M. A. Jensen, "Termination-dependent diversity performance of coupled antennas: network theory analysis," *IEEE Transactions on Antennas and Propagation*, vol. 52, no. 1, pp. 98–105, 2004.

[9] J. Weber, C. Volmer, K. Blau, R. Stephan, and M. A. Hein, "Miniaturisation of antenna arrays for mobile communications," in *Proceedings of the 35th European Microwave Conference*, pp. 1173–1176, Paris, France, October 2005.

[10] J. Weber, C. Volmer, K. Blau, R. Stephan, and M. A. Hein, "Miniaturized antenna arrays using decoupling networks with realistic elements," *IEEE Transactions on Microwave Theory and Techniques*, vol. 54, no. 6, pp. 2733–2740, 2006.

[11] J. Weber, C. Volmer, K. Blau, R. Stephan, and M. A. Hein, "Implementation of a miniaturized antenna array with predefined orthogonal radiation patterns," in *Proceedings of the European Conference on Antennas and Propagation (EuCAP '06)*, pp. 1–5, Nice, France, November 2006.

[12] A. Krewski, W. L. Schroeder, and K. Solbach, "Matching network synthesis for mobile MIMO antennas based on minimization of the total multi-port reflectance," in *Proceedings of the 7th Loughborough Antennas and Propagation Conference (LAPC '11)*, pp. 1–4, Loughborough, UK, November 2011.

[13] A. Krewski and W. L. Schroeder, "N-port DL-MIMO antenna system realization using systematically designed mode matching and mode decomposition network," in *Proceedings of the 2012 42nd European Microwave Conference (EuMC '12)-Held as Part of 15th European Microwave Week (EuMW '12)*, pp. 156–159, Amsterdam, Netherlands, November 2012.

[14] F. Broydé and E. Clavelier, "Some properties of multiple-antenna-port and multiple-user-port antenna tuners," *IEEE Transactions on Circuits and Systems I: Regular Papers*, vol. 62, no. 2, pp. 423–432, 2015.

[15] F. Broydé and E. Clavelier, "A new multiple-antenna-port and multiple-user-port antenna tuner," in *Proceedings of the IEEE Radio & Wireless Week (RWW '15)*, pp. 41–43, San Diego, Calif, USA, January 2015.

[16] F. Broydé and E. Clavelier, "Two multiple-antenna-port and multiple-user-port antenna tuners," in *Proceedings of the 9th European Conference on Antennas and Propagation (EuCAP '15)*, Lisbon, Portugal, April 2015.

[17] R. A. Horn and C. R. Johnson, *Matrix Analysis*, Cambridge University Press, Cambridge, UK, 2nd edition, 2013.

[18] R. A. Horn and C. R. Johnson, *Topics in Matrix Analysis*, Cambridge University Press, Cambridge, UK, 1991.

[19] *The A. R. R. L. Antenna Book*, The American Radio Relay League, 8th edition, 1956.

[20] R. G. Vaughan and J. B. Andersen, "Antenna diversity in mobile communications," *IEEE Transactions on Vehicular Technology*, vol. 36, no. 4, pp. 149–172, 1987.

[21] S. Stein, "On cross coupling in multiple-beam antennas," *IRE Transactions on Antennas and Propagation*, vol. 10, no. 5, pp. 548–557, 1962.

[22] K. Wang, L. Li, and T. F. Eibert, "Estimation of signal correlation of lossy compact monopole arrays with decoupling networks," *IEEE Transactions on Antennas and Propagation*, vol. 63, no. 1, pp. 357–363, 2015.

[23] W.-K. Chen, Ed., *The Circuits and Filters Handbook*, CRC Press/IEEE Press, 1995.

[24] US patent no. 5,564,086, "Method and apparatus for enhancing an operating characteristic of a radio transmitter," Filed: November 29, 1993.

[25] U.S. patent no. 6,414,562, "Circuit and method for impedance matching," Filed: May 27, 1997.

[26] International application no. PCT/IB2015/057161, "Method for automatically adjusting a tuning unit, and automatic tuning system using this method," Priority: French patent application 15/01780 of 26 August 2015.

[27] Y. Sun and J. K. Fidler, "Design of Π impedance matching networks," in *Proceedings of the IEEE International Symposium on Circuits and Systems*, vol. 5, pp. 5–8, London, UK, June 1994.

[28] Q. Gu, J. R. De Luis, I. Morris, and J. Hilbert, "An analytical algorithm for pi-network impedance tuners," *IEEE Transactions on Circuits and Systems I. Regular Papers*, vol. 58, no. 12, pp. 2894–2905, 2011.